

AD-A203 202

4

AD

TECHNICAL REPORT ARCCB-TR-88040

**MICROSCOPIC ASPECTS OF FAILURE  
AND FRACTURE IN CROSS-PLY FIBER-  
REINFORCED COMPOSITE LAMINATES**

**S. BANDYOPADHYAY**

**V. M. SILVA**

**E. P. GELLERT**

**J. H. UNDERWOOD**

**S** DTIC  
ELECTE  
DEC 21 1968  
**D**  
D

NOVEMBER 1968



**US ARMY ARMAMENT RESEARCH,  
DEVELOPMENT AND ENGINEERING CENTER  
CLOSE COMBAT ARMAMENTS CENTER  
BENET LABORATORIES  
WATERVLIET, N.Y. 12180-4050**



APPROVED FOR PUBLIC RELEASE; DISTRIBUTION UNLIMITED

88 12 21 058

**DISCLAIMER**

The findings in this report are not to be construed as an official Department of the Army position unless so designated by other authorized documents.

The use of trade name(s) and/or manufacturer(s) does not constitute an official indorsement or approval.

**DESTRUCTION NOTICE**

For classified documents, follow the procedures in DoD 5200.22-M, Industrial Security Manual, Section II-19 or DoD 5200.1-R, Information Security Program Regulation, Chapter IX.

For unclassified, limited documents, destroy by any method that will prevent disclosure of contents or reconstruction of the document.

For unclassified, unlimited documents, destroy when the report is no longer needed. Do not return it to the originator.



7. AUTHORS (CONT'D)

S. Bandyopadhyay, E. P. Gellert, and V. M. Silva  
Materials Research Laboratories  
Defence Science and Technology Organisation  
P.O. Box 50  
Ascot Vale, Victoria, 3032  
Australia

20. ABSTRACT (CONT'D)

This report emphasizes the microscopic deformation processes and seeks to explain (1) the superior tensile fracture toughness of a commercial laminate of the new composite system carbon/bismaleimide over a commercial laminate of the conventional material carbon/epoxy, and (2) the dependence of interlaminar failure in glass and carbon fiber/epoxy laminates on the fracture energy of the matrix resin.

UNCLASSIFIED

TABLE OF CONTENTS

	<u>Page</u>
ACKNOWLEDGEMENT .....	iii
INTRODUCTION AND SCOPE .....	1
MATERIALS AND METHODS .....	2
Tensile Fracture Studies .....	2
Interlaminar Fracture Studies .....	3
Fracture Surface Examination .....	6
RESULTS AND DISCUSSION .....	6
Tensile Fracture .....	6
Interlaminar Fracture .....	11
CONCLUSIONS.....	16
REFERENCES .....	17

TABLES

I. TENSILE FRACTURE MATERIALS AND TEST RESULTS .....	3
II. INTERLAMINAR MATERIALS AND FRACTURE ENERGIES .....	5

ILLUSTRATIONS

1. Experimental arrangement for tensile fracture testing of composites .....	4
2. Interlaminar fracture testing using the width-tapered double-cantilever beam specimen .....	6
3. Typical load-displacement diagram for tensile fracture .....	7
4. Fracture surface of carbon/epoxy showing little fiber pull-out .....	9
5. Fracture surface of carbon/bismaleimide showing extensive pull-out .....	9
6. Carbon/epoxy showing clustering without any appreciable debonding .....	9

	<u>Page</u>
7. Carbon/bismaleimide showing debonding and pull-out of individual fibers .....	9
8. Load-displacement traces of the interlaminar fracture specimens .....	12
9. Fiber bridging in glass/828-DDS interlaminar fracture .....	13
10. Delamination failure .....	14
11. Resin-rich region, glass/828-DDS .....	14
12. Resin-lean area, glass/828-DDS .....	14
13. Ductile matrix failure, carbon/828-DDS .....	14
14. Brittle failure, carbon/MY720-DDS .....	15

## ACKNOWLEDGEMENT

The authors wish to acknowledge the help of the following Materials Research Laboratories staff: Mr. I. A. Burch for performing the tensile fracture tests; Dr. Brian Ennis for providing the DSC results; and Mr. Gary Mathys for IR analysis of the resins in the carbon/epoxy and the carbon/bismaleimide tensile fracture specimens; and Dr. Jim Brown for valuable comments on the manuscript. We also wish to acknowledge the help of Mr. William Yaiser of Benet Laboratories in preparing the carbon/epoxy and carbon/bismaleimide specimens.

## INTRODUCTION AND SCOPE

Two aspects of the failure of fiber-reinforced composite materials which have received considerable attention in the literature are tensile fracture of laminates with a notch or a precrack (refs 1,2) and interlaminar fracture of composites under mode I loading conditions (refs 3-5). Linear elastic fracture mechanics principles have been applied in both cases to assess the composite fracture properties in terms of the critical stress intensity factor,  $K_{Ic}$ , or the critical strain energy release rate,  $G_{Ic}$ . The effect of matrix properties on the bulk fracture behavior has been investigated and fracture surfaces have been examined by scanning electron microscopy (SEM) (refs 4-6).

The important energy-absorbing mechanisms in tensile fracture of composites include: (1) multiple cracking of fibers, (2) matrix cracking, (3) fiber-matrix interfacial debonding, and (4) fiber pull-out and frictional shear separation (ref 7). While it is difficult to estimate the relative contribution of these processes to the tensile fracture toughness of a composite laminate, debonding and pull-out, which depend on the fiber-matrix interface characteristics, can play a very significant role.

Interlaminar fracture (delamination) is recognized as an important mode of failure of composite materials because interlaminar defects can be induced easily by low energy impact or during the manufacture of composite panels, and growth of these defects can occur under load. Therefore, interlaminar fracture energy,  $G_{Ic}$ , may be used as a measure of damage tolerance in composites.  $G_{Ic}$  depends on the matrix fracture energy, fiber-matrix interfacial bond, degree of crack branching and deviation, fiber bridging across the crack faces, and also fiber pull-out (refs 3,8).

---

References are listed at the end of this report.

The choice of matrix materials is considered to be an important factor in the ultimate fracture properties of the laminate. However, matrix properties do not seem to have a significant influence on the tensile composite fracture toughness, at least in random fiber composites (ref 9). In contrast, the interlaminar fracture energy has been reported to increase progressively with increased matrix fracture energy (ref 5).

This report presents the results of experiments on (1) tensile fracture of commercial cross-ply laminates of carbon/epoxy and carbon/bismaleimide, and (2) interlaminar fracture of carbon/epoxy and glass/epoxy woven laminates. The tensile fracture of carbon/epoxy is compared with that of carbon/bismaleimide, a new class of composites with the matrix resin having moderately high glass transition temperatures ( $T_g$ ), between 200° and 400°C (ref 10). The interlaminar fracture study is important because it involves matrix cracking and interfacial separation for which the fracture energy is much lower than for tensile fracture. Thus, interlaminar fracture is often a performance-limiting parameter. In both sets of experiments, the correlation between the microscopic aspects of deformation and the macroscopic fracture behavior has been studied to develop an understanding of the micromechanisms of the failure process.

## **MATERIALS AND METHODS**

### **Tensile Fracture Studies**

The carbon/epoxy composite used was in the form of cured sheets, consisting of 7 plies supplied by 3M Company, ply type SP-285/T2. Both 0-degree and 90-degree fibers were low modulus, high strength type. The carbon/bismaleimide laminate of 11 plies was prepared from Fiberite X-86 prepreg tape, cured at 180°C and 170 kPa for 4 hours, followed by post-curing at 240°C for 6 hours. The 0-degree fibers in the laminate were high strength, whereas the 90-degree

fibers were high modulus types.

Infrared (IR) spectroscopy and differential scanning calorimetry (DSC) of the cured laminates were carried out to obtain information about the resin composition and other characteristics. The epoxy used was identified as Ciba-Geigy MY720 (TGMDA) (ref 11) cured with diamino diphenyl sulphone (DDS). DSC studies indicated that both laminates were fully cured. The  $T_g$  of the epoxy was about 200°C and that for the bismaleimide was about 220°C.

The fracture toughness,  $K_{Ic}$ , of the laminates was obtained using center-notched specimens, shown in Figure 1, and the following expression for stress intensity factor K (ref 12):

$$KBW^{3/2}/P = [\pi a/W \sec (\pi a/W)]^{1/2}$$

for  $0 < 2a/W < 0.9$  ,  $H/W > 0.75$  (1)

where P = load at failure. Some details of the specimens and properties are given in Table I.

TABLE I. TENSILE FRACTURE MATERIALS AND TEST RESULTS

Material	Orientation degrees	Width (W) mm	Thickness (B) mm	$K_{Ic}$ ; Mean of 3 MPa m <sup>1/2</sup>	Standard Deviation MPa m <sup>1/2</sup>
Carbon/Epoxy	90,0,90,0	100	1.13	16.6	1.6
Carbon/Bismaleimide	90,0,90,0,90,0	90	1.78	45.3	2.3

#### Interlaminar Fracture Studies

The laminates for these experiments were prepared from woven cloth fabric using the resins Shell Epikote 828 (DGEBA) (ref 11) cured with DDS, and Ciba-Geigy MY720 cured with DDS. The Epikote 828 was used as the matrix with (1) a carbon fabric, Fothergill and Harvey style A004, 7 x 7 cm and (2) a glass fabric

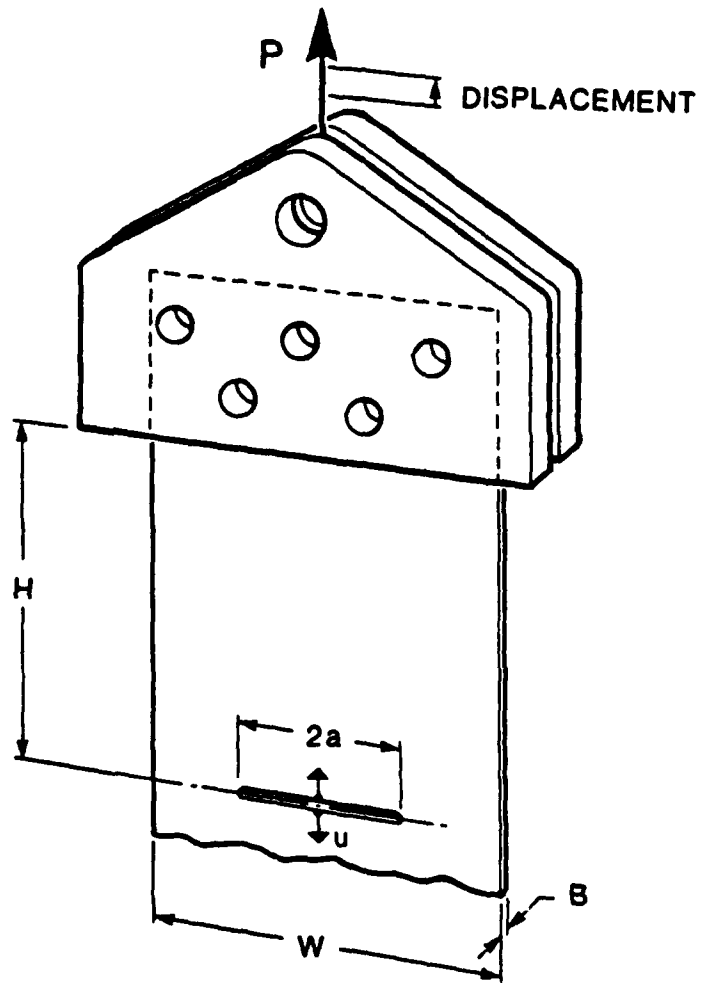


Figure 1. Experimental arrangement for tensile fracture testing of composites.

S-2 glass, Owens Corning 6781. The cure schedule for the 828-DDS composites was 5 hours at 120°C, 550 kPa, then 19 hours at 120°C, and 4 hours at 180°C. The MY720-DDS was used as the matrix with the Fothergill and Harvey carbon fabric only, and was cured for 4 hours at 120°C, 550 kPa, then 2 hours at 175°C. The compositions of the resins and the composites are given in Table II.

TABLE II. INTERLAMINAR MATERIALS AND FRACTURE ENERGIES

Material	Method	G <sub>IC</sub> ; Mean of 4-6 J/m <sup>2</sup>	Standard Deviation J/m <sup>2</sup>
*Epikote 828 (DGEBA)/DDS, 32 phr.	DT	128	11
**MY720 (TGMDA)/DDS, 29 phr.	DT	39	-
**30 ply carbon fabric: Epikote 828-DDS Fiber 55% v/v	WTDCB	770	87
**30 ply carbon fabric: MY720-DDS Fiber 60% v/v	WTDCB	470	36
**40 ply S-2 glass fabric: Epikote 828-DDS Fiber 50% v/v	WTDCB	812	110

\*neat cured resin

\*\*composite

The critical strain energy release rate, G<sub>IC</sub>, was determined for the neat resin using double torsion (DT) specimens (ref 13). The interlaminar fracture toughness for the composites, also considered a G<sub>IC</sub> value, was obtained using the width-tapered double-cantilevered beam (WTDCB) specimens (ref 4), shown in Figure 2, and the following expression for strain energy release rate, G (ref 12):

$$G = K^2/E = \frac{12P^2a^2}{Eh^3b^2}, \quad a \gg h \quad (2)$$

where P = load to propagate an interlaminar crack and E = bending modulus of the composite measured from three-point bend tests. Equation (2) is most accurate

for plane-stress conditions and for a large ratio of crack length to specimen height,  $a/h$ . For the conditions of the interlaminar crack growth tests here, it is believed to give a reasonable estimate of fracture toughness (ref 4).

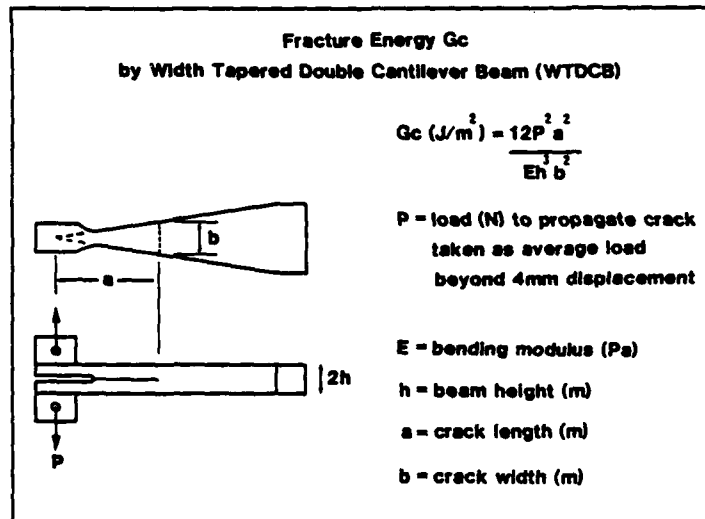


Figure 2. Interlaminar fracture testing using the width-tapered double-cantilever beam specimen.

### Fracture Surface Examination

This was carried out after coating fractured specimens with gold in a Cambridge S250 stereo-scan mark 2 scanning electron microscope with secondary electrons.

## RESULTS AND DISCUSSION

### Tensile Fracture

The load-displacement characteristics of the laminates were as follows. The carbon/epoxy laminate showed essentially linear behavior, while the carbon/bismaleimide composite showed deviation from linearity (Figure 3) of about the degree associated with high strength metals, followed by abrupt failure. Thus, linear elastic fracture mechanics can be used to describe the tensile fracture

behavior. The  $K_{IC}$  for the two laminates, obtained from Eq. (1), is given in Table I. The carbon/epoxy laminate has an average  $K_{IC}$  of  $16.6 \text{ MPa m}^{1/2}$  which agrees well with published values obtained from center-notched specimens of carbon/epoxy laminates of similar orientation ( $20.1 \text{ MPa m}^{1/2}$ ) (ref 14).

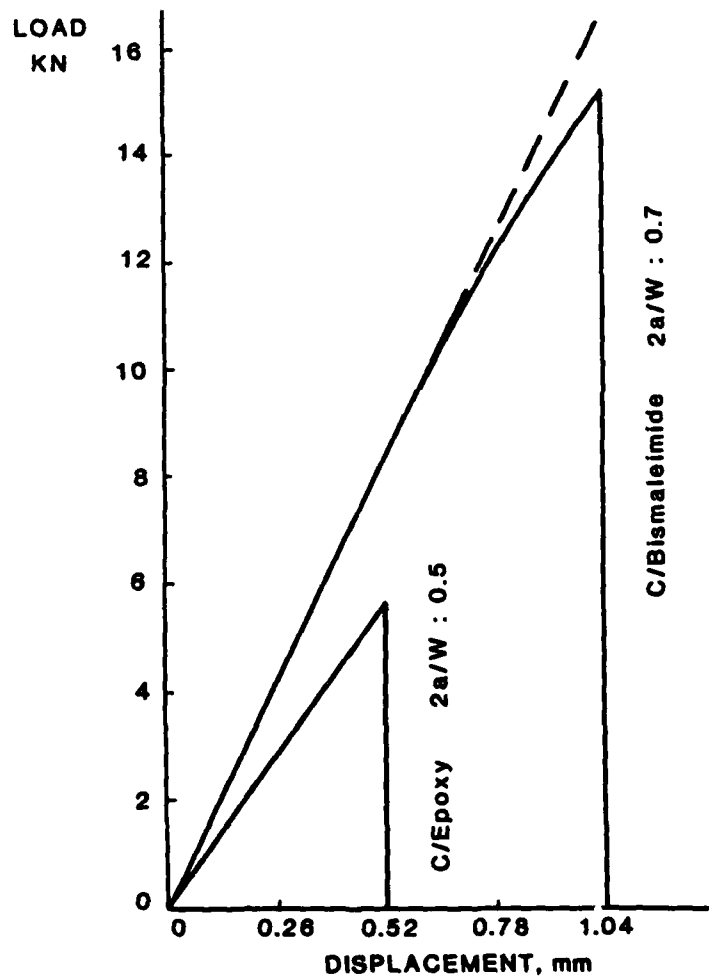


Figure 3. Typical load-displacement diagram for tensile fracture.

The carbon/bismaleimide composite, on the other hand, has an average  $K_{IC}$  of 45.3 MPa  $m^{1/2}$  which is more than 2½ times greater than that of carbon/epoxy, and in terms of  $G_{IC}$ , this difference is approximately 6½ times, following Eq. (2).

Since the two laminates were obtained from commercial sources, adequate information is not available regarding the fiber and matrix characteristics. However, since the 0-degree fibers in both laminates are the high strength type, it is assumed that the fiber properties are not much different. Further, the matrix  $G_{IC}$  of the two resins can be different (40 J/m<sup>2</sup> for the epoxy and 30-200 J/m<sup>2</sup> for the bismaleimide (ref 10)), but the effect of this difference in  $G_{IC}$  on the tensile fracture toughness of the laminates may not be significant (ref 9) as stated earlier.

In order to investigate the significant difference in fracture properties, fracture surfaces of the carbon/epoxy and carbon/bismaleimide composites were examined and are shown in Figures 4 through 7. The low magnification fracture surface of carbon/epoxy appears rather smooth (Figure 4), while that for carbon/bismaleimide appears 'fibrous' (Figure 5). The high magnification fracture surface of the carbon/epoxy laminate (Figure 6) suggests minimal evidence of fiber pull-out, and even if some pull-out has occurred, it was in a cluster. (Similar fracture surfaces have been observed in other studies of carbon/epoxy laminates (ref 6).) In contrast, fracture of carbon/bismaleimide shows distinct evidence of individual fiber pull-out (Figure 7). From visual observation, the pull-out length varied between 1 and 3 mm, and the debonded zone length between the notch tip and failure edge averaged 9 mm.

When the 0-degree fibers are loaded in tension, the difference in the stress levels in fibers and matrix (due to the difference in modulus) creates a shear stress along the interfaces. When this stress exceeds the fiber-matrix

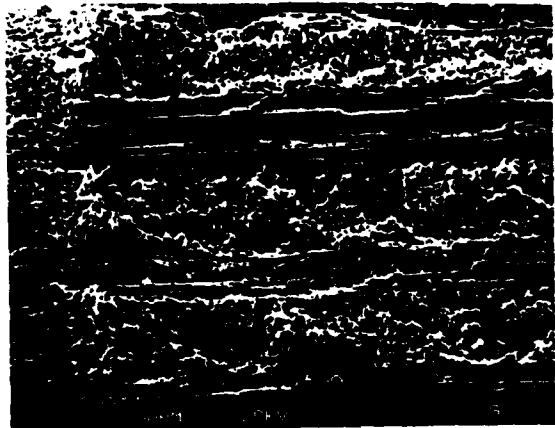


Figure 4. Fracture surface of carbon/epoxy showing little fiber pull-out.

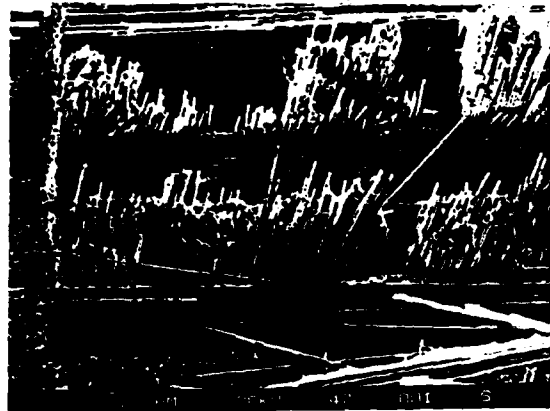


Figure 5. Fracture surface of carbon/bismaleimide showing extensive pull-out.



Figure 6. Carbon/epoxy showing clustering without any appreciable debonding.



Figure 7. Carbon/bismaleimide showing debonding and pull-out of individual fibers.

interfacial shear strength, debonding takes place. The debonding stress ( $\sigma_d$ ) is a function of the interfacial shear energy ( $G_{II}$ ):  $\sigma_d \propto (G_{II})^{1/2}$ . Debonding is itself a major energy-absorbing mechanism, but once debonding takes place, the subsequent work of fracture depends upon: (1) elastic energy in the fiber, (2) surface energy of the newly created interface, and (3) work of fiber pull-out that depends on the diameter of the fiber, frictional shear, and length of pull-out.

In continuous fiber composites, a low interfacial shear energy favors fiber-matrix debonding. This was experimentally verified by Kirk et al. (ref 15) who observed preferential pull-out of glass fibers in glass and carbon hybrid/epoxy composites where the interface energy for glass/epoxy was 210 J/m<sup>2</sup>, much lower than for carbon/epoxy, 1950 J/m<sup>2</sup> (ref 7). Comparison of this work with the present SEM observations (Figures 4 through 7) suggests that the possible mechanism that makes carbon/bismaleimide tougher is the debonding and large pull-out length, whereas for carbon/epoxy composites the toughness is primarily derived from the frictional work to extract short lengths of broken fibers out of the cracked matrix (ref 16). An estimate of the debonding energy ( $\gamma_d$ ) and pull-out energy ( $\gamma_p$ ) for the carbon/bismaleimide composite can be made by using the pull-out model of Kirk et al. (ref 15) as follows:

$$\gamma_d = \frac{\sigma_f^2 y}{4E_f} \quad , \quad \gamma_p = \frac{\sigma_f l}{24}$$

where

$\sigma_f$  = tensile strength of the fiber

$E_f$  = elastic modulus of the fiber

$y$  = length of the debond zone

$l$  = critical length = 4 x length of pull-out

Using typical data for carbon fiber,  $\sigma_f = 2.4$  GPa and  $E_f = 240$  GPa, and from visual observation,  $y = 9$  mm (average) and  $l = 4 \times 2$  mm (average), for carbon/bismaleimide

$$\gamma_d = 216 \text{ kJ/m}^2 \quad \text{and} \quad \gamma_p = 800 \text{ kJ/m}^2$$

which are much higher than those reported for carbon/epoxy (ref 15)

$$\gamma_d = 6 \text{ kJ/m}^2 \quad \text{and} \quad \gamma_p = 110 \text{ kJ/m}^2$$

Further, the fracture surface of carbon/epoxy (Figure 6) is similar to the proposed model of pull-out of fiber-clusters by Bandyopadhyay and Murthy (ref 17). When significant clustering occurs, the energy absorbed in the separation process can be as low as 10 to 25 percent of the total energy required by pull-out of individual fibers. Thus, this model can also partially explain the difference in fracture toughness of carbon/epoxy and carbon/bismaleimide composites in the present study.

#### Interlaminar Fracture

The load-displacement traces for interlaminar fracture of the three composite laminates are shown in Figure 8. Once crack initiation takes place at the end of the linear region, propagation of the crack proceeds in a stick-slip manner. Stick-slip crack growth, which can be used as a measure of the localized crack-tip plastic deformation (ref 18), was prominent in the glass/828-DDS laminate, and it was just visible in the carbon/MY720-DDS composite.

The mode I interlaminar fracture energy,  $G_{IC}$ , for the composite laminates, obtained using Eq. (2) and taking  $P$  as the average load beyond 4-mm displacement (Figure 8), is given in Table II. Also given in Table II is the neat resin  $G_{IC}$  for 828-DDS and MY720-DDS. It is clear from these values that MY720-DDS is a brittle resin in comparison to 828-DDS, and correspondingly the interlaminar fracture energy for carbon/MY720-DDS laminate is considerably less than that of the carbon/828-DDS.

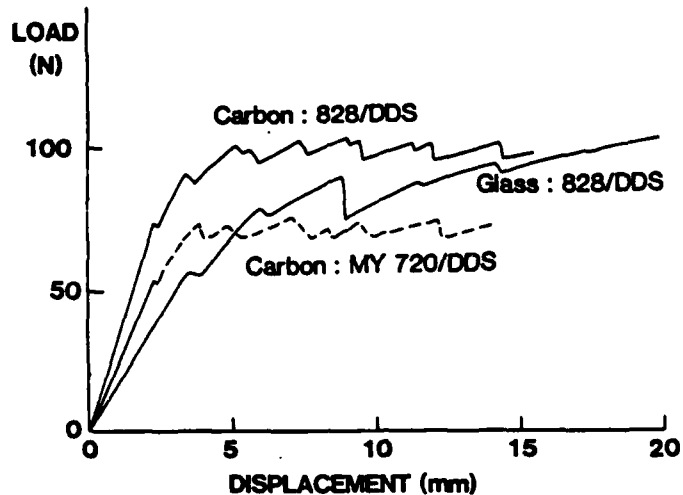


Figure 8. Load-displacement traces of the interlaminar fracture specimens.

Some aspects of these results agree with those reported by Hunston (ref 5). A tougher resin results in a higher interlaminar  $G_{IC}$ . The fibers in continuous fiber laminated composites contribute significantly to the interlaminar fracture energy by fiber breakage, pull-out, and fiber bridging of the crack, resulting in a much higher  $G_{IC}$  than for the bulk resin. For the carbon and glass composites with 828-DDS, the different reinforcement has not caused significant differences in interlaminar  $G_{IC}$ , suggesting a higher dependence here on resin fracture energy than on reinforcement type.

Crack branching and the related fiber bridging were observed with each of the three composites, but they were most pronounced with the glass fabric as shown in Figure 9 involving a whole ply bridged across the crack opening in three stick-slip sequences. The photo sequence in Figure 9 was taken with a high-speed camera.

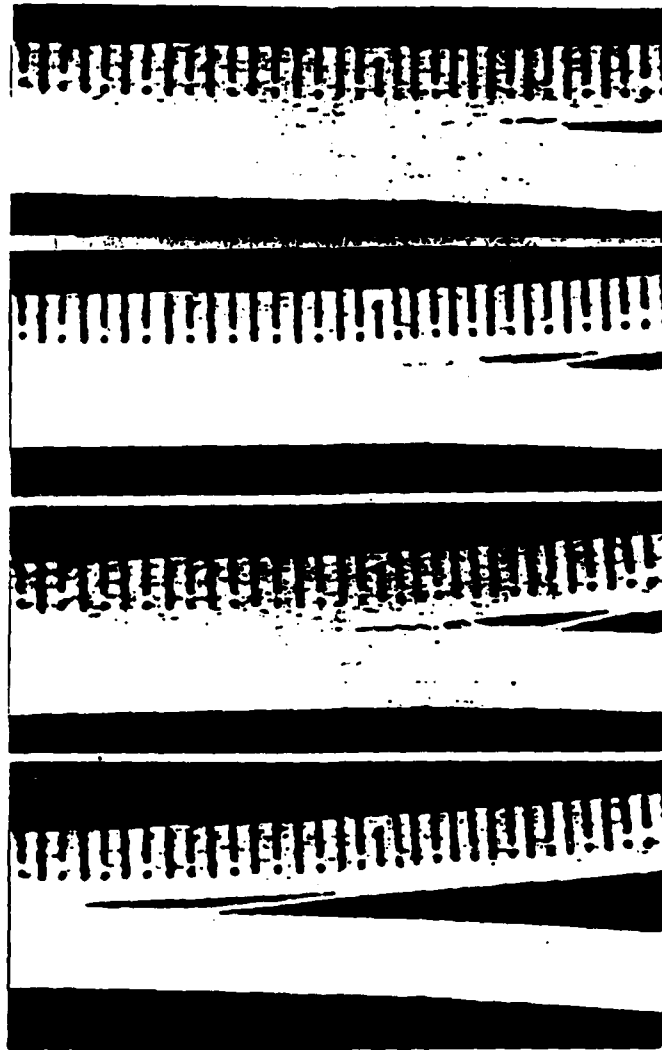


Figure 9. Fiber bridging in glass/828-DDS interlaminar fracture.

Examination of fracture surfaces of the laminates was carried out to understand the micromechanisms of this type of fracture. Figure 10 shows a low magnification view of the general delamination. At high magnification, the glass composite fracture surfaces feature contrasting resin-rich regions (Figure 11) and resin-lean fiber bundles where the crack appears to have deviated from the matrix between plies to a location within plies (Figure 12). There is some evidence of localized plastic deformation in the matrix of carbon/828-DDS composite (Figure 13), while the fracture surface of the carbon/MY720-DDS shows cleaner failure (Figure 14) consistent with the brittle nature of the neat resin.



Figure 10. Delamination failure.

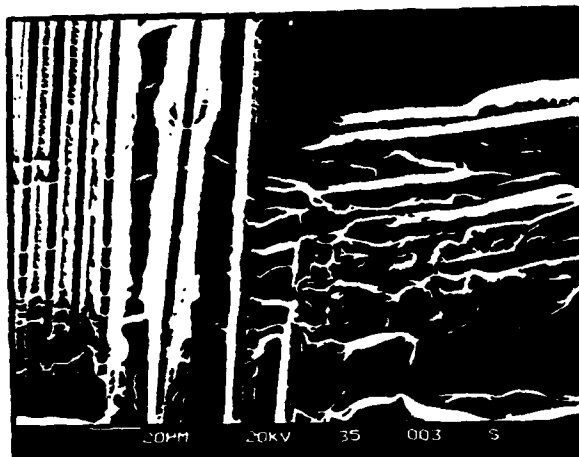


Figure 11. Resin-rich region, glass/828-DDS.



Figure 12. Resin-lean area, glass/828-DDS.

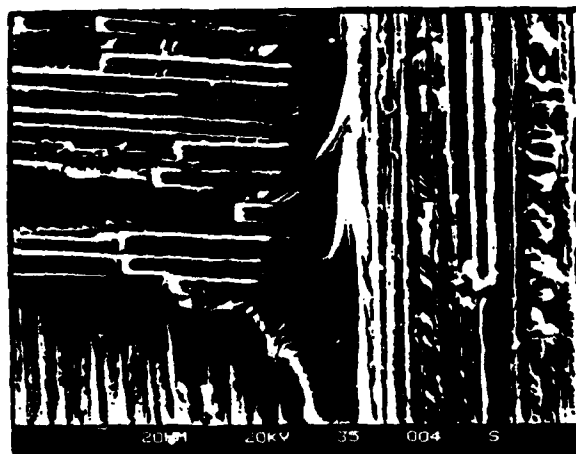


Figure 13. Ductile matrix failure, carbon/828-DDS.

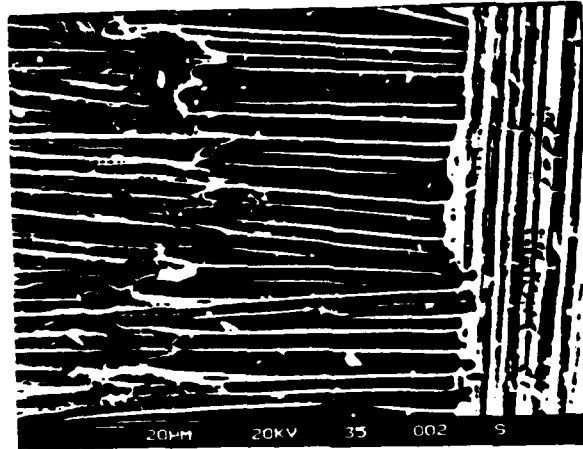


Figure 14. Brittle failure, carbon/MY720-DDS.

Although the effect of resin  $G_{IC}$  on the interlaminar  $G_{IC}$  of the composite has been studied experimentally and reported in the literature (ref 5), no attempt has been made so far to correlate the characteristic crack-tip plastic zone size of the bulk resin to the size of the resin ligament in the composite. The radius of the theoretical plane-strain crack-tip plastic zone ( $r_y$ ) of the matrix can be calculated as

$$r_y = \frac{G_{IC}E}{6\pi\sigma_y^2} \quad (3)$$

where  $E$  and  $\sigma_y$  are the elastic modulus and yield strength of the bulk resin.

Using representative values for  $E$  and  $\sigma_y$ ,  $r_y$  for the 828-DDS and MY720-DDS resins can be calculated at 2.7 and 0.8  $\mu\text{m}$ . Figures 13 and 14 indicate that the resin ligaments between the fibers range in size from about 3 to 8  $\mu\text{m}$ . One interpretation is that if the matrix layer is significantly thinner than  $r_y$ , then the crack-tip plastic zone is constricted, which would not allow sufficient crack-tip blunting and would therefore reduce toughness. The matrix layer here appears to accommodate the characteristic plane-strain plastic zone size for

these two resins and this could possibly explain how the matrix fracture energy can influence the composite interlaminar  $G_{IC}$ .

#### CONCLUSIONS

1. In tensile fracture studies, the carbon/bismaleimide laminate showed significantly higher toughness than the carbon/epoxy composite. This is attributed to extensive debonding and pull-out of individual fibers in carbon/bismaleimide and the virtual absence of the same mechanism in carbon/epoxy.

2. The bulk fracture energy of the resin makes a direct contribution to the interlaminar fracture energy of the composite. However, other factors such as crack branching and crack bridging also can absorb energy.

3. In interlaminar fracture, the characteristic plane-strain plastic zone size of the bulk resin may influence the interlaminar fracture energy of the composite.

## REFERENCES

1. M. E. Waddoups, J. R. Eisenmann, and B. E. Kaminski, "Macroscopic Fracture Mechanics of Advanced Composite Materials," J. Composite Materials, Vol. 5, October 1971, p. 446.
2. C. G. Aronsson and J. Backlund, "Tensile Fracture of Laminates With Cracks," J. Composite Materials, Vol. 20, No. 3, May 1986, p. 287.
3. J. M. Scott and D. C. Phillips, "Carbon Fibre Composites With Rubber Toughened Matrices," J. Materials Science, Vol. 10, No. 4, April 1975, p. 551.
4. W. D. Bascom, J. L. Bitner, R. J. Moulton, and A. R. Siebert, "The Interlaminar Fracture of Organic-Matrix Woven Reinforced Composites," Composites, Vol. 11, No. 1, January 1980, p. 9.
5. D. L. Hunston, "Composite Interlaminar Fracture: Effect of Matrix Fracture Energy," Composites Technology Review, Vol. 6, No. 4, 1984, p. 176.
6. D. Purslow, "Some Fundamental Aspects of Composites Fractography," Composites, Vol. 12, No. 4, October 1981, p. 241.
7. J. K. Wells and P. W. R. Beaumont, "Fracture Energy Maps for Fibre Composites," J. Materials Science, Vol. 17, No. 2, February 1982, p. 397.
8. A. J. Russell and K. N. Street, in: Progress in Science and Engineering of Composites, Vol. 1, Japan Society for Composite Materials, 1982, p. 279.
9. B. D. Agarwal and L. J. Broutman, Analysis and Performance of Fiber Composites, Wiley-Interscience, 1980.
10. D. A. Scola, "The Status of Bismaleimides for Composites," Proc. ICCM V, (W. C. Harrigan, Jr., J. Strife, and A. K. Dhingra, eds.), The Metallurgical Society, Inc., 1985, p. 1601.
11. C. A. May and Y. Tanaka, eds., Epoxy Resins - Chemistry and Technology, Marcel Dekker, Inc., NY, 1973.
12. H. Tada, P. C. Paris, and G. R. Irwin, The Stress Analysis of Cracks Handbook, Del Research Corporation, Hellertown, PA, 1973.
13. S. Yamini and R. J. Young, "Stability of Crack Propagation in Epoxy Resins," Polymer, Vol. 18, October 1977, p. 1075.
14. T. H. Mao, "Tensile Fracture of Graphite/Epoxy Laminates With Central Crack," Proc. ICCM V, (W. C. Harrigan, Jr., J. Strife, and A. K. Dhingra, eds.), The Metallurgical Society, Inc., 1985, p. 383.
15. J. N. Kirk, M. Munro, and P. W. R. Beaumont, "The Fracture Energy of Hybrid Carbon and Glass Fibre Composites," J. Materials Science, Vol. 13, No. 10, October 1978, p. 2197.

16. P. W. R. Beaumont and B. Harris, "The Energy of Crack Propagation in Carbon Fibre-Reinforced Resin Systems," J. Materials Science, Vol. 7, No. 11, November 1972, p. 1265.
17. S. Bandyopadhyay and P. N. Murthy, "Experimental Studies on Interfacial Shear Strength in Glass Fibre Reinforced Plastics Systems," Materials Science and Engineering, Vol. 19, No. 1, May 1975, p. 139.
18. S. Bandyopadhyay, "Fracture Mechanisms of Structural Epoxies," Presented at the 6th Polymer Technology Convention, Canberra, October 1982; the Australasian Section of Plastics and Rubber Institute.

TECHNICAL REPORT INTERNAL DISTRIBUTION LIST

	<u>NO. OF COPIES</u>
CHIEF, DEVELOPMENT ENGINEERING BRANCH	
ATTN: SMCAR-CCB-D	1
-DA	1
-DC	1
-DM	1
-DP	1
-DR	1
-DS (SYSTEMS)	1
CHIEF, ENGINEERING SUPPORT BRANCH	
ATTN: SMCAR-CCB-S	1
-SE	1
CHIEF, RESEARCH BRANCH	
ATTN: SMCAR-CCB-R	2
-RA	1
-RM	1
-RP	1
-RT	1
TECHNICAL LIBRARY	5
ATTN: SMCAR-CCB-TL	
TECHNICAL PUBLICATIONS & EDITING UNIT	3
ATTN: SMCAR-CCB-TL	
DIRECTOR, OPERATIONS DIRECTORATE	1
ATTN: SMCWV-OD	
DIRECTOR, PROCUREMENT DIRECTORATE	1
ATTN: SMCWV-PP	
DIRECTOR, PRODUCT ASSURANCE DIRECTORATE	1
ATTN: SMCWV-QA	

**NOTE:** PLEASE NOTIFY DIRECTOR, BENET LABORATORIES, ATTN: SMCAR-CCB-TL, OF ANY ADDRESS CHANGES.

TECHNICAL REPORT EXTERNAL DISTRIBUTION LIST

	<u>NO. OF COPIES</u>		<u>NO. OF COPIES</u>
ASST SEC OF THE ARMY RESEARCH AND DEVELOPMENT ATTN: DEPT FOR SCI AND TECH THE PENTAGON WASHINGTON, D.C. 20310-0103	1	COMMANDER ROCK ISLAND ARSENAL ATTN: SMCRI-ENM ROCK ISLAND, IL 61299-5000	1
ADMINISTRATOR DEFENSE TECHNICAL INFO CENTER ATTN: DTIC-FDAC CAMERON STATION ALEXANDRIA, VA 22304-6145	12	DIRECTOR US ARMY INDUSTRIAL BASE ENGR ACTV ATTN: AMXIB-P ROCK ISLAND, IL 61299-7260	1
COMMANDER US ARMY ARDEC ATTN: SMCAR-AEE	1	COMMANDER US ARMY TANK-AUTMV R&D COMMAND ATTN: AMSTA-DDL (TECH LIB) WARREN, MI 48397-5000	1
SMCAR-AES, BLDG. 321	1	COMMANDER	
SMCAR-AET-O, BLDG. 351N	1	US MILITARY ACADEMY	1
SMCAR-CC	1	ATTN: DEPARTMENT OF MECHANICS	
SMCAR-CCP-A	1	WEST POINT, NY 10996-1792	
SMCAR-FSA	1		
SMCAR-FSM-E	1	US ARMY MISSILE COMMAND	
SMCAR-FSS-D, BLDG. 94	1	REDSTONE SCIENTIFIC INFO CTR	2
SMCAR-IMI-I (STINFO) BLDG. 59	2	ATTN: DOCUMENTS SECT, BLDG. 4484	
PICATINNY ARSENAL, NJ 07806-5000		REDSTONE ARSENAL, AL 35898-5241	
DIRECTOR US ARMY BALLISTIC RESEARCH LABORATORY ATTN: SLCBR-DD-T, BLDG. 305	1	COMMANDER US ARMY FGN SCIENCE AND TECH CTR ATTN: DRXST-SD	1
ABERDEEN PROVING GROUND, MD 21005-5066		220 7TH STREET, N.E. CHARLOTTESVILLE, VA 22901	
DIRECTOR US ARMY MATERIEL SYSTEMS ANALYSIS ACTV ATTN: AMXSY-MP	1	COMMANDER US ARMY LABCOM	
ABERDEEN PROVING GROUND, MD 21005-5071		MATERIALS TECHNOLOGY LAB	
COMMANDER HQ, AMCCOM ATTN: AMSMC-IMP-L	1	ATTN: SLCMT-IML (TECH LIB)	2
ROCK ISLAND, IL 61299-6000		WATERTOWN, MA 02172-0001	

**NOTE:** PLEASE NOTIFY COMMANDER, ARMAMENT RESEARCH, DEVELOPMENT, AND ENGINEERING CENTER, US ARMY AMCCOM, ATTN: BENET LABORATORIES, SMCAR-CCB-TL, WATERVLIET, NY 12189-4050, OF ANY ADDRESS CHANGES.

TECHNICAL REPORT EXTERNAL DISTRIBUTION LIST (CONT'D)

	<u>NO. OF COPIES</u>		<u>NO. OF COPIES</u>
COMMANDER US ARMY LABCOM, ISA ATTN: SLCIS-IM-TL 2800 POWDER MILL ROAD ADELPHI, MD 20783-1145	1	COMMANDER AIR FORCE ARMAMENT LABORATORY ATTN: AFATL/MN EGLIN AFB, FL 32542-5434	1
COMMANDER US ARMY RESEARCH OFFICE ATTN: CHIEF, IPO P.O. BOX 12211 RESEARCH TRIANGLE PARK, NC 27709-2211	1	COMMANDER AIR FORCE ARMAMENT LABORATORY ATTN: AFATL/MNF EGLIN AFB, FL 32542-5434	1
DIRECTOR US NAVAL RESEARCH LAB ATTN: MATERIALS SCI & TECH DIVISION CODE 26-27 (DOC LIB) WASHINGTON, D.C. 20375	1 1	METALS AND CERAMICS INFO CTR BATTELLE COLUMBUS DIVISION 505 KING AVENUE COLUMBUS, OH 43201-2693	1

**NOTE:** PLEASE NOTIFY COMMANDER, ARMAMENT RESEARCH, DEVELOPMENT, AND ENGINEERING CENTER, US ARMY AMCCOM, ATTN: BENET LABORATORIES, SMCAR-CCB-TL, WATERVLIET, NY 12189-4050, OF ANY ADDRESS CHANGES.